



**HAL**  
open science

# Ensuring long-term stability of infrared camera absolute calibration

A. Kattnig, S. Thetas, J. Primot

► **To cite this version:**

A. Kattnig, S. Thetas, J. Primot. Ensuring long-term stability of infrared camera absolute calibration. Optics Express, 2015, 23 (14), p. 18381-18390. 10.1364/OE.23.018381 . hal-01229474

**HAL Id: hal-01229474**

**<https://hal.science/hal-01229474>**

Submitted on 16 Nov 2015

**HAL** is a multi-disciplinary open access archive for the deposit and dissemination of scientific research documents, whether they are published or not. The documents may come from teaching and research institutions in France or abroad, or from public or private research centers.

L'archive ouverte pluridisciplinaire **HAL**, est destinée au dépôt et à la diffusion de documents scientifiques de niveau recherche, publiés ou non, émanant des établissements d'enseignement et de recherche français ou étrangers, des laboratoires publics ou privés.

# Ensuring long-term stability of infrared camera absolute calibration

Alain Kattnig,<sup>1,\*</sup> Sophie Thetas,<sup>1</sup> and Jérôme Primot<sup>1</sup>

<sup>1</sup>Office National d'Etudes et de Recherche Aéronautique, Département d'Optique Théorique et Appliquée, Chemin de la Hunière, 91761 Palaiseau cedex, France

\*alain.kattnig@onera.fr

**Abstract:** Absolute calibration of cryogenic 3-5  $\mu\text{m}$  and 8-10  $\mu\text{m}$  infrared cameras is notoriously instable and thus has to be repeated before actual measurements. Moreover, the signal to noise ratio of the imagery is lowered, decreasing its quality. These performances degradations strongly lessen the suitability of Infrared Imaging. These defaults are often blamed on detectors reaching a different “response state” after each return to cryogenic conditions, while accounting for the detrimental effects of imperfect stray light management. We show here that detectors are not to be blamed and that the culprit can also dwell in proximity electronics. We identify an unexpected source of instability in the initial voltage of the integrating capacity of detectors. Then we show that this parameter can be easily measured and taken into account. This way we demonstrate that a one month old calibration of a 3-5  $\mu\text{m}$  camera has retained its validity.

©2015 Optical Society of America

**OCIS codes:** (150.1488) Calibration; (110.3080) Infrared imaging; (110.4280) Noise in imaging systems; (120.3940) Metrology; (120.0280) Remote sensing and sensors; (040.1240) Arrays; (040.2480) FLIR, forward-looking infrared.

---

## References and links

1. G. C. Holst, *Testing and Evaluation of Infrared Imaging Systems* (SPIE Optical Engineering Press, 1998), p. 53.
2. J. F. Johnson, “Hybrid infrared focal plane signal and noise model,” *IEEE Trans. Electron. Dev.* **46**(1), 96–108 (1999).
3. S. Thetas, S. Bernhardt, M. Caes, C. Coudrain, P. Cymbalista, J. Deschamps, and J. Primot, “SIELETTERS: a static Fourier transform infrared imaging spectrometer for airborne hyperspectral measurements,” in *Sensors and Electronics Panel (SET) Specialists*, Brussels, Belgium (2009).
4. G. Ohring, J. Tansock, W. Emery, J. Butler, L. Flynn, F. Weng, and T. Stone, “Achieving Satellite Instrument Calibration for Climate Change (ASIC 3),” Report of a Workshop at the National Conference Center, Lansdowne, VA, May 16–18 (2006).
5. E. Friedman and J. L. Miller, *Photonics Rules of Thumbs*, 2nd ed. (McGraw-Hill, 2003), p. 289.
6. S. L. Lawson, B. M. Jakosky, H. S. Park, and M. T. Mellon, “Brightness temperatures of the lunar surface: Calibration and global analysis of the Clementine long-wave infrared camera data,” *J. Geophys. Res.* **105**, E2 (2000).
7. S. W. Brown, T. C. Larason, C. Habauzit, G. P. Eppeldauer, Y. Ohno, and K. R. Lykke, “Absolute radiometric calibration of digital imaging systems,” *Photonics West 2001-Electronic Imaging*, (International Society for Optics and Photonics, 2001).
8. P. W. Kruse, *Uncooled Thermal Imaging: Arrays, Systems, and Applications*, Vol. 2003 (SPIE Press, 2001).
9. P. W. Nugent, J. A. Shaw, and N. J. Pust, “Correcting for focal-plane-array temperature dependence in microbolometer infrared cameras lacking thermal stabilization,” *Opt. Eng.* **52**(6), 061304 (2013).
10. Y. Cao and C. L. Tisse, “Shutterless solution for simultaneous focal plane array temperature estimation and nonuniformity correction in uncooled long-wave infrared camera,” *Appl. Opt.* **52**(25), 6266–6271 (2013).
11. www.winlight-system.com
12. X. Brenière, L. Rubaldo, and F. Dupont, “Sofradir's recent improvements regarding the reliability and performance of HgCdTe IR detectors,” *SPIE Defense + Security* (International Society for Optics and Photonics, 2014).
13. C. Coudrain, S. Bernhardt, M. Caes, R. Domel, Y. Ferrec, R. Gouyon, D. Henry, M. Jacquart, A. Kattnig, P. Perrault, L. Poutier, L. Rousset-Rouvière, M. Tauvy, S. Thétas, and J. Primot, “SIELETTERS, an airborne infrared dual-band spectro-imaging system for measurement of scene spectral signatures,” *Opt. Express* **23**(12), 16164–16176 (2015).
14. K. Rank, M. Lendl, and R. Unbehauen, “Estimation of image noise variance,” *IEE P-Vis. Image Sign.* **146**(2), 80–84 (1999).

15. S. Torres, R. Reeves, and M. Hayat, "Scene-based nonuniformity correction method using constant-range: Performance and analysis," *Proceedings of 6th World Multiconference on Systemics, Cybernetics and Informatics*, **9** (2002).
- 

## 1. Introduction

Calibration of infrared cameras is too often considered as an engineering task and thus is seldom subject of academic developments. Nevertheless this last step of instrument set-up, by giving the level of the residual spatial noise in the image, often the dominant source of noise, drives directly the final signal to noise ratio of cameras in several wavelength domains.

We study here the long-term stability of calibrations in the infrared domain for cryogenic detectors technologies such as HgCdTe or InSb, which retain the crown for best radiometric performances.

It is well-known that the best use of instruments built around these kinds of detectors needs a lengthy process of calibration using blackbodies [1] which can't always be used in the exact geometric configuration of the working instrument. Indeed such process is readily available on laboratories but much less so on the field where less effective equipments are often used. And prospects are bleak for airborne equipment, since it is often impossible to put blackbodies and collimators below or near a "live" aircraft or helicopter.

Part of this calibration volatility is rightly credited to imperfect stray light management and imperfect temperature control of the focal plane array, but the remainder is usually blamed on an unexplainable hysteresis arising between thermal cycles of the detector.

We show here that detectors are not to be blamed and we switch the blame towards too stringent requirements on proximity electronics of the detectors and the Readout Integrated Circuit (ROIC) [2]. Then we present a very simple model of calibration in which we introduce an important but overlooked parameter, the initial voltage offset of the reading circuit, able to capture part of the variability plaguing infrared imaging.

Next we study the performance of this model on our recently developed airborne imaging spectrometer, called Sieleters [3], a cooled HgCdTe-based instrument operating simultaneously in the 3-5  $\mu\text{m}$  and 8-11  $\mu\text{m}$  infrared domains.

We will show that it is possible, under some hypothesis, to retain an absolute calibration for a long time and to obtain in-flight radiometric performances on par with those measured in laboratory. Remember that, for example, the reliability of absolute infrared measures is a strong goal of climatic science [4].

## 2. The detector and the read-out circuit

The heart of the infrared camera being the detector, we show in Fig. 1 a sketch of the "standard" circuitry of a single detector element. Whatever the chosen technology, the photo-detector will either create or modify an electric current that will charge or discharge an electrical capacity. In turn, its value will be read by an external electronic, converted into a numerical format and made available to its user.

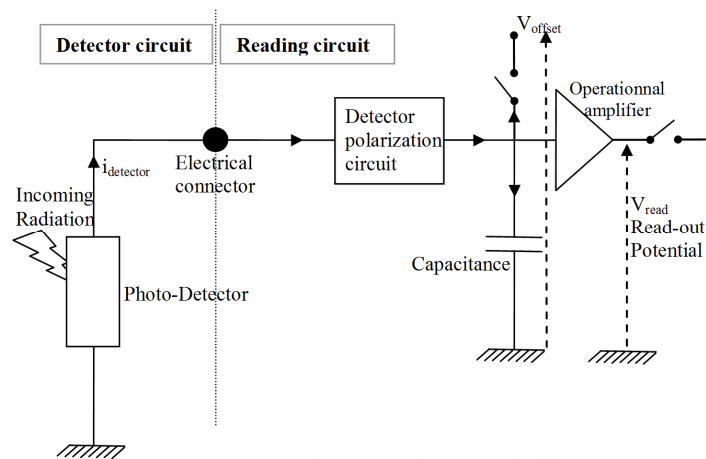


Fig. 1. Simplified electrical model of a light-sensitive detector and its associated reading circuit.

Circuit designers aim for the best linear response possible and can achieve very high shunt resistivities. Thus, for non-exotic designs, the following measurement equation will hold:

$$V_{read} = \frac{i_{detector} (T_{detector}, \text{Radiance})}{C} \times t_i + V_{initial} + V_{Noise} \quad (1)$$

We give in Table 1 the significance of parameters of Eq. (1).

**Table 1. Parameters of the circuit of radiation measurement**

$V_{Read}$	Measured voltage
$T_{detector}$	Current operating temperature of the detector
$Radiance$	Incoming radiance on the detector
$i_{detector}$	Electrical current running through the detector circuit
$t_i$	Integration time
$C$	Capacitance of the integrating capacity
$V_{initial}$	Initial voltage of the capacity.
$V_{Noise}$	Temporal noise affecting voltage measurements.

### 3. Absolute radiometric calibration

Since the measured voltage is affine versus the incoming photometric radiance, it is in theory quite straightforward to convert the measured voltage into radiance by using calibrating blackbodies.

A minimum of two different blackbody temperatures are then necessary to retrieve this relation, even if more temperatures would provide a more robust relation. *In fine*, this relation allows the conversion of the voltage output into an “equivalent” integrated radiance measured at the blackbody location.

#### 3.1 Calibration of arrays of detectors

This procedure of calibration might then be used in arrays of detectors, by calibrating each detector individually. But this straightforward solution leads to a spatial noise much higher than the temporal noise. This is not an impediment for an absolute radiometric measure, notoriously difficult to make (even laboratory blackbodies are only radiometrically accurate up to a few percent in infrared bands [5]), but this noise will lower the quality of curves or images thus acquired in which we look for spatial information, such as shapes.

This spatial noise arises from small disparities in spectral transmission, bandwidth and quantum efficiency. Unfortunately, the precise experimental measure of these parameters is a very difficult task.

Fortunately, the spatial homogeneity of the blackbodies radiance is very good, often much higher than the radiometric resolution of the camera to calibrate. Thus in practice the real challenge in such a calibration lies in the spatial homogenization of the response of detectors submitted, by hypothesis, to identical radiances. Indeed, contrary to the “invisible” absolute radiometric error, imperfect homogenizations are very conspicuous.

To our knowledge [6,7], this homogenization has mostly been based on finding an optimal affine transformation of the output of each detector versus a “reference” pixel output, given in Eq. (2).

$$V_{reference\ detector}(T_{Blackbody}) = g_i \times V_{detector\ i}(T_{Blackbody}) + o_i \quad (2)$$

$V_{reference\ detector}$  being the voltage output of a reference pixel and  $V_{detector\ i}$  being the voltage output of any other detector.

$g_i$  and  $o_i$  are computed by a least square regression analysis between the two sets of voltage output indexed on the temperature of the blackbody shown in front of the camera. The noise voltage component has been dropped, since measures are strongly averaged to guarantee a negligible noise voltage power.

Once the array of detector has been spatially homogenized, the absolute calibration is simply obtained as in the previous section by calibrating the reference detector, since all corrected detectors now should behave identically.

### 3.2 Drawbacks

Infrared imaging has long been plagued by the temporal instability of this homogenization process [1]. It means frequent calibrations and thus the transportation on the field of a lot of equipments, including blackbodies and collimators for long focal imaging systems. Furthermore, a different calibration is needed for each integration time. All of which limits the use of infrared cameras.

This situation is usually thought to be a by-product of imperfect stray light management, due to variable emissions of internal parts of the camera and to some hysteresis occurring in detectors between thermal cycle (for cooled detectors).

Builders of cooled and uncooled infrared cameras, have started to use the measure of internal temperature of cameras by creating a set of calibration parameters for each different recorded temperature of the camera. Thus it is possible to manage the worst of temporal evolution of cameras [8]. For such commercial products which don't always have very rigorous stray light designs, the improvement is spectacular [9,10], thus demonstrating the importance of either controlling or modelling stray light.

Nevertheless, it is still necessary to fully understand the origin of these temporal instabilities, should we hope to make absolute measures. And since the two Sieleters infrared cameras have been designed around a tight control of stray light, it is the opportunity to study its efficiency.

## 4. Absolute radiometric calibration based on the photo-current and consequences

All these points can be completely or partially addressed by the model of correction we propose. We have seen that, traditionally, calibrations are directly performed on the measured electrical voltage output of the detector capacitance fed by a photo-current which is linearly linked to the incoming radiance. To our knowledge most of published works on infrared calibration have been based on the use of this voltage [1,6,7].

But, it is always interesting to work as close as possible to the signal we seek to measure, the incoming infrared radiation. And since this radiation drives directly the photo-current of the electrical circuit of Fig. 1, we will use this current instead of the voltage. Which gives the following relation in Eq. (3).

$$i_{k,l}^{Circuit} = C_{k,l} \times \frac{V_{k,l}^{Read} - V_{k,l}^{Initial}}{t_{integration}} \quad (3)$$

[k,l] being indices of the individual detector, assumed in this case to be a matrix.

This photo-current can be further divided into three components, the current induced by the radiance of the observed scene, the current induced by stray light and the dark current coming from thermally excited electrons entering the conduction band, given in Eq. (4).

$$i_{k,l}^{Circuit} = i_{k,l}^{Scene} + i_{k,l}^{Stray\ lighth} + i_{k,l}^{Dark} \quad (4)$$

When a blackbody of uniform radiance is shown in front of the camera, we can write the following invariant quantity, in Eq. (5):

$$\forall (k,l) \quad \frac{i_{k,l}^{Scene}}{\eta_{k,l} \times G_{k,l}} = constant \quad (5)$$

$\eta_{k,l}$  being the spectral quantum efficiency of the detector of indices [k,l] and  $G_{k,l}$  the étendue defined between each detector and the exit pupil it sees.

By selecting a “reference” detector [ $k_0, l_0$ ] in the previous quantity, we obtain the following relation between the currents of all other detectors, in Eq. (6):

$$i_{k_0, l_0}^{Circuit} = \underbrace{\frac{\eta_{k_0, l_0} \times G_{k_0, l_0}}{\eta_{k,l} \times G_{k,l}}}_{g_{k,l}} \times i_{k,l}^{Circuit} + \underbrace{\left[ i_{k_0, l_0}^{Stray\ lighth} + i_{k_0, l_0}^{Dark} \right] - \frac{\eta_{k_0, l_0} \times G_{k_0, l_0}}{\eta_{k,l} \times G_{k,l}} \times \left[ i_{k,l}^{Stray\ lighth} + i_{k,l}^{Dark} \right]}_{o_{k,l}} \quad (6)$$

This equation demonstrates the adequacy of using an affine correction in Eq. (2). And it demonstrates for the first time the negative correlation arising between the affine parameters, given Eq. (7).

$$o_{k,l} = \left[ i_{k_0, l_0}^{Stray\ lighth} + i_{k_0, l_0}^{Dark} \right] - g_{k,l} \times \left[ i_{k,l}^{Stray\ lighth} + i_{k,l}^{Dark} \right] \quad (7)$$

There is an important consequence of this property: if the shape of  $g_{k,l}$  is nowhere to be found in  $o_{k,l}$ , meaning no correlation, it indicates that the camera doesn't suffer from extraneous signals. The two possibilities are illustrated in Fig. 2 and Fig. 3 on a real instrument.

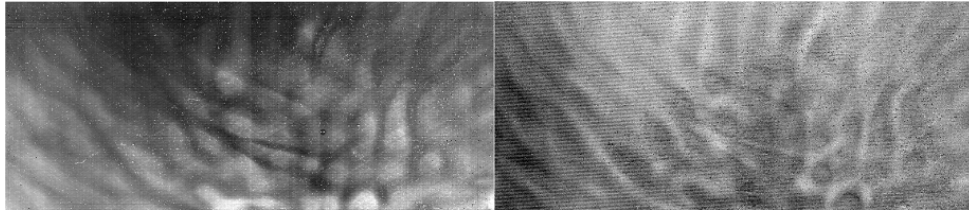


Fig. 2. Sialeters band III parameters of homogenization,  $g_{k,l}$  on the left and  $o_{k,l}$  on the right. An inverse correlation is clear.

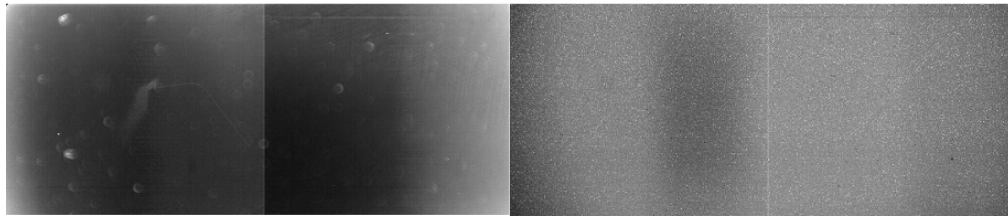


Fig. 3. Sialeters band II parameters of affine correction,  $g_{k,l}$  on the left and  $o_{k,l}$  on the right. The absence of disk-like structures on the right demonstrates the very low level of extraneous signals in this infrared band, which is expected.

These results justify and explain a long standing practice of affine correction in calibration, see Eq. (3). But the use of the current highlights an interesting parameter often

overlooked since it “hides” naturally in the relative offset parameter,  $o_{k,l}$ . It is the initial voltage of the capacity in Eq. (1):  $V_{\text{initial}}$ .

Naturally, after having performed this relative correction, a traditional calibration of the reference detector with all available blackbody measurements is calculated and allows the recovery of the observed luminance.

#### *4.1 Catching all or part of the temporal variability of the correction of the camera*

Indeed, the calculation of the current of the reading circuit needs the knowledge of the capacitance of each detector, of the integration time and of the initial voltage of the capacity.

In practice, the measure of the individual capacitance is both troublesome and unnecessary since its variations can easily be integrated in the relative gain,  $g_{k,l}$ . The average value will then be used to give a good estimate of the current.

The integration time is, since it is set, very well known. There remains the initial voltage of each capacity which is reset each time the final voltage had been read by electrically connecting them to a voltage source. This last parameter is very interesting, since it is easily and quickly measured by setting a zero integration time on the reading circuit.

Better still, on an ideally built infrared imaging camera this parameter might contain all remaining sources of variability since, to our knowledge, this parameter hasn't yet been considered as an important source of temporal variability in relation with radiometric stability.

Actually, a 50 mK control of detector temperature means no variations of quantum efficiency, which in turn means no variation of the relative gain. Cryogenically regulated camera innards and good stray light management mean that the parasitic radiance will stay constant, thus the relative offset should also stay constant. This means that the Sieleters instrument is the perfect tool to test our idea.

### **5. Experimental set-up and in flight radiometric performances of the Sieleters instruments**

The 3-5  $\mu\text{m}$  and 8-11  $\mu\text{m}$  Sieleters imaging spectrometers [3] have been calibrated in laboratory respectively in October 2013, the 16th and the 23rd in front of a very compact collimator specifically designed for us by Winlight Systems [11] in front of a laboratory-class blackbody at its focal plane. We used a CI Systems SR-80-7A blackbody with an emissivity of  $0.97 \pm 0.02$  on the [3 $\mu\text{m}$ -12 $\mu\text{m}$ ] spectral range. Between twelve and fifteen different temperatures were thus measured, ranging from 15 °C to 70 °C and using several integration times. The initial voltage has also been measured. The HgCdTe detector arrays were built specifically by Sofradir [12] and put into a cryocooler at 60K.

In flight, two measures of the initial voltage have been taken, one before the actual acquisition process and the second after. Additional details about the instrument are available in reference [13].

#### *5.1 The MWIR camera*

The relative gain and offset measured in laboratory and the corresponding absolute calibration, see Fig. 2 and Fig. 3, have been used to calibrate the airborne observation campaign acquired the 25th of September 2013 near the French city of Toulouse. But it remains to choose which measurement of in-flight initial voltage we should use before applying the laboratory calibration. Three different measures of initial voltage are available, one acquired one month later in laboratory, another one taken 50 minutes before the acquisition process and the last one taken 30 minutes after the acquisition.

We give Fig. 4 a comparison between uses of these different parameters.

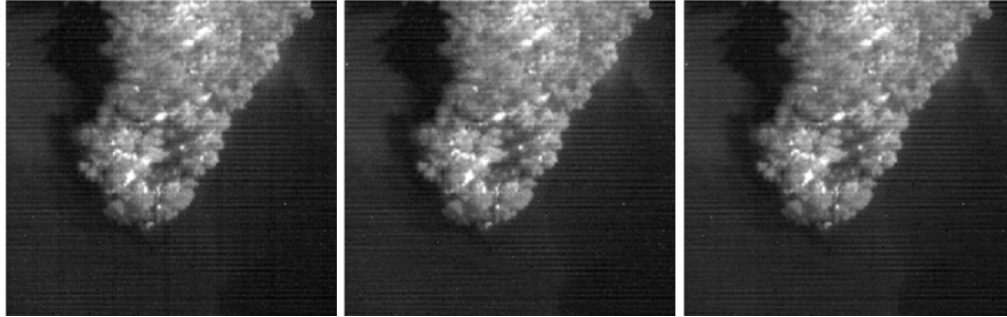


Fig. 4. Left, image close-up obtained by using the initial voltage of the reading circuit obtained in laboratory, notice the vertical lines. Center, the same image calibrated by the initial voltage taken 50 mn before. Right, the image calibrated by the initial voltage taken 30 mn after. The integration time is 1.5 ms and the capacity used can hold two millions electrons.

Horizontal fringes are a feature of these interferometric images, see Fig. 4, and contain spectral information [3,13], contrary to the vertical lines plaguing the left image. Thus the use of a one-month old voltage leads to the appearance of verticals measured at 0.3 pA amplitude (almost three times the temporal noise at 0.11 pA), while the use of the much more recent two initial voltages doesn't have any visible impact on the local image quality.

And radiometric biases are much higher; we give Fig. 5 the difference between the initial voltage measured in laboratory and the one measured just at the beginning of the flight.

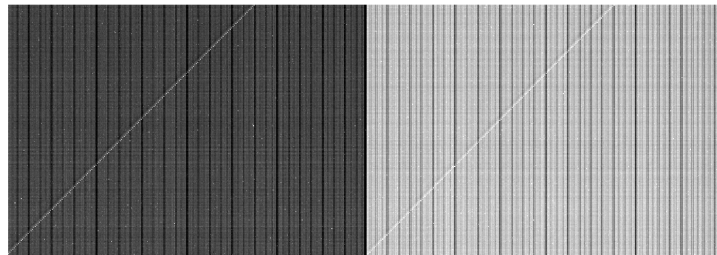


Fig. 5. Difference between the initial voltage measured at the beginning of the flight and the initial voltage measured one month later on laboratory. Converted in current, the range on the left part is  $[-0.8, -0.5]$  pA while on the right it is  $[-0.5, -0.3]$  pA with a minimum at the center at  $-1$  pA.

Translated in equivalent temperature, the step-like bias is 0.4 K high, a noticeable radiometric error, since it is seven times higher than the temporal noise and thus quite conspicuous.

Even if the resulting local image quality is satisfactory, the two initial voltage measurements made in flight reveal an evolution. Their difference is very similar in shape to the one given Fig. 5, but with values divided by three: verticals have only an amplitude 0.1 pA while the absolute offset is between 0 and 0.3 pA. It implies that initial voltage measurements closer to the actual time of acquisition would be preferable.

At last, the total noise, estimated on a smooth part of the right image of Fig. 4 by a method of difference [14], is 0.125 pA, very near the measured temporal noise value of 0.11 pA.

Thus we have demonstrated that by using our calibration scheme based on photo-current calibration and a “last minute” measure of the initial voltage, we were able to operate a MWIR camera with no in situ calibration at a signal to noise ratio very near the maximum, with less than 0.15 K radiometric biases (for a NETD of 65 mK at 20°C) and no noticeable imagery artefacts. Nevertheless we'll certainly be able to further reduce biases by measuring the initial voltage closer to the actual acquisition.

A classical voltage-based calibration would have been unable to catch these image impairments and would have been oblivious to such biases.

## 5.2 The LWIR camera

This camera has been calibrated under the same conditions as its MWIR counterpart and they have flown together. Three initial voltage measurements are also available, one taken one month later in laboratory, another one taken 12 minutes before the acquisition process and the last one taken 61 minutes after the acquisition.

Unfortunately, in this case, none of these measurements are able to sufficiently correct the acquisition. Indeed, the fact that two different reading circuits are mounted on the matrix of detector becomes readily apparent, see Fig. 6. We measured between these half-circuits a contrast of 24 pA by using the initial voltage measured in laboratory, 18 pA for the pre-acquisition voltage and 10 pA with the post-acquisition voltage.

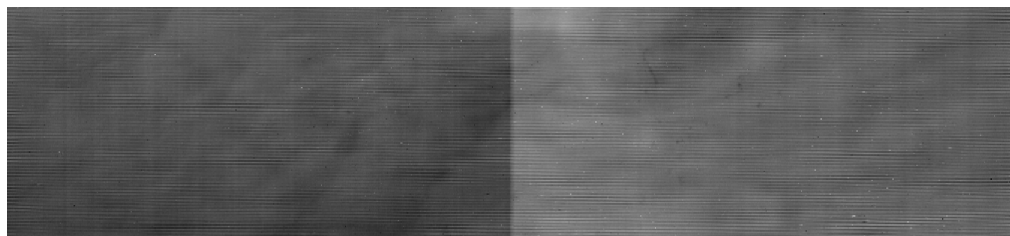


Fig. 6. Part of an image over a river measured by the LWIR Sieleters camera using an initial voltage measured 12 minutes before taking this image. Notice the sharp contrast denoting a dissimilar voltage evolution between the two reading circuits. The radiometric range used is 50 pA wide and the contrast is 18 pA, corresponding to 20 times the noise standard deviation and an equivalent temperature contrast of 1K. The image mean is 1.6 nA.

This contrast is quite sizeable since the temporal noise is only 0.9 pA. And like its MWIR counterpart, this contrast is separated in two halves, see Fig. 7, whose position matches the layout of the two electrical sources used to initialize capacities initial voltage.

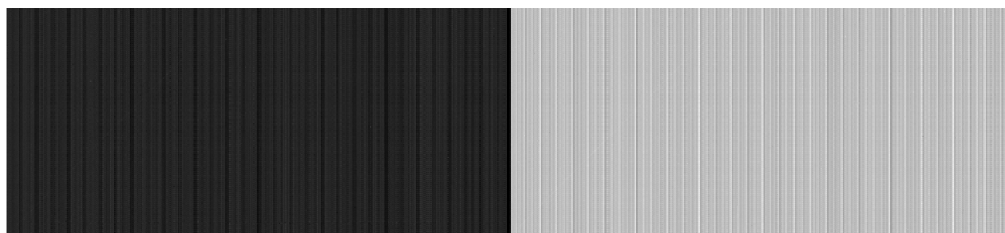


Fig. 7. Difference of the two in-flight measures of the initial voltage of the LWIR array of detector. The two halves have different averages, separated by 3 mV or 8 pA, and exhibit a 4 columns period.

We can also find in this figure the 4 columns period which is linked to the 4 different electrical outputs used to read each half array of detectors. Each output being a different electrical circuit, discrepancies of voltage are expected and easy to correct, but what is needed is a temporal stability in the range of a few hundred of microvolts (corresponding to the temporal noise). Such stability is extremely difficult to ensure on an airborne instrument and might explain the offset shown Fig. 6 as well as a potentially much greater radiometric bias.

But this time, we have seen that our measures of the initial voltage aren't sufficient to catch these voltage variations. They also lead to a noise three times higher than the temporal noise at 2.6 pA. The step-like offset and the faint verticals seen Fig. 6 resembles those of Fig. 7 proving that they come from the ROIC and the detector driving electronics.

The reason of this behavior discrepancy between MWIR and LWIR lies within the size of the charge-integrating capacity, since it has to be nearly twenty times as large for the LWIR imager compared with MWIR. This is in part because of the greater photon count in LWIR band but also because of the large dark current plaguing high wavenumber photo-detectors.

These two phenomena lead to a greater sensibility of the current measurement to voltage instabilities, see Eq. (1) and the impact of increasing the capacity  $C$ . That's what is experienced here.

Thus, in the future, we will measure the initial voltage just before the start of an acquisition. But unless we opt for taking an initial voltage measure before each image, we must show that a 42 seconds acquisition process is short enough to escape variations of the initial voltage.

### 5.3 Post-acquisition evaluation of voltage offset

There are numerous methods using scene statistics to correct images suffering from fixed-pattern noise [15]. We elected to use such a solution to find out if there exists a valid offset correction for the whole acquisition. And it turned out that it is successful enough, see Fig. 8, to catch the “step” effect as well as to lower the fixed-pattern noise below the temporal noise of 0.9 pA.

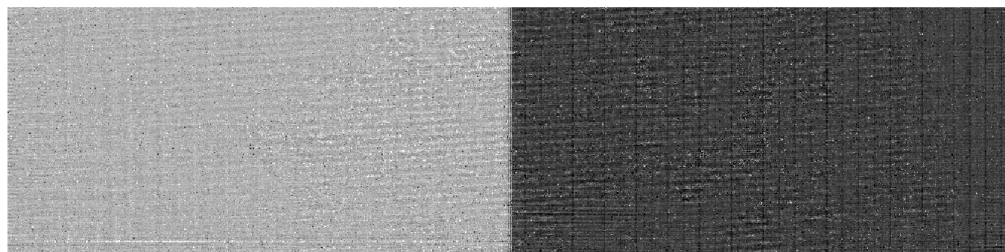


Fig. 8. Correcting offset used to remove the artefacts in the original image of Fig. 6 and to reduce the noise. The strong step separating the two halves of the circuit is well measured. After application of this correcting offset, the residual noise becomes equal to the temporal noise.

Thus, since we have been able to correct the fixed-pattern noise, it proves that, on the timescale of the 42 seconds-long acquisition, this noise is stable enough. Therefore, it is highly probable that a measure of the initial voltage much closer to the actual time of acquisition will be able to correct a large part the variability incurring in the read-out circuit.

Besides, we detected after the flight a faulty welding in the ROIC that could explain the unexpected variation and magnitude of these instabilities. All in all, we can expect to mostly offset the variability of the initial voltage of detector capacity.

In any case we have, for now, shown the importance of the measure of the initial voltage of the detector capacity when looking for the best radiometric quality of measure, both relative and absolute.

## 6. Perspectives

We have scheduled laboratory measures of blackbody to study the long term absolute stability of our instrument thus utilized. We have also scheduled a measure of initial voltage just before and after the actual acquisition and are looking forward to our next flight to check its efficiency.

And we are working to extract an indirect measure of extraneous signal from the coefficients of spatial homogenization.

## 7. Conclusions

We have shown that by working on the current coursing the circuit of a photo-detector, a quantity directly infused by the incoming radiation, we gain useful insights on the spatial homogenization process. In particular the optimality of the affine correction has been proved and we have found in this correction an indirect way to detect stray light, without being yet able to quantify it, yet.

Then, we have shown that by measuring the initial voltage of the detector capacity, a very easy experimental measurement, we are able to offset part or all of the variability usually plaguing infrared imaging.

In practice, this measure allows our Sieleters MWIR camera to operate without any calibration on the field and we have good reason to believe that our LWIR camera won't require a calibration as well, by adjusting our experimental process.

### **Acknowledgment**

The authors would like to express their thanks to Christophe Coudrain and the whole Sieleters team responsible for the design, building and operating the instrument and who made it available for other uses. We also want to thank the Direction Générale de l'Armement (the French Ministry of Defense) for his interest in this work.